Journal of Molecular Structure 1227 (2021) 129550

Contents lists available at ScienceDirect

Journal of Molecular Structure

journal homepage: www.elsevier.com/locate/molstr

Investigations substituent effect on structural, spectral and optical properties of phenylboronic acids

Burcu Çöpçü, Koray Sayin*, Duran Karakaş

Sivas Cumhuriyet University, Faculty of Science, Department of Chemistry, 58140 Sivas, TURKEY

ARTICLE INFO

Article history:
Received 29 September 2020
Revised 29 October 2020
Accepted 29 October 2020
Available online 30 October 2020

Keywords:
Boron
Spectral Analysis
NLO Properties
Arylboronic acid

ABSTRACT

Ortho- and para-substituent arylboronic acid are investigated. Geometric structure and structural properties of these compounds are done. IR and NMR spectrum are calculated for the spectral characterizations. Contour diagram of frontier molecular orbitals which are HOMO and LUMO is calculated and molecular electrostatic potential (MEP) map of them are obtained to evaluate the electronic properties and to determine the active site on the molecules. Non-linear optical (NLO) properties are investigated. UV–VIS spectrum of studied compounds is calculated and the wavelength of main band is examined. Then, some quantum chemical parameters which are total static dipole moment, the average linear polarizability, the anisotropy of the polarizability and first hyperpolarizability are calculated and it was found that B3 is the best NLO material for applications.

1. Introduction

Arylboronic acids are significant compound group due to the fact that they have broad application areas. Although these compounds have been known over more than a hundred years, their properties and application areas are still expanding even today. The most known significant areas are the synthesis of biaryl compounds, molecular receptor, organic framework especially covalent and bioactivity of them [1-8]. The substituent and its location on the phenyl ring are gained significant effect on the acidity, receptor activity, and biological activity, etc. The other important research area is optic. It is known that optical properties of boron compounds have been investigated in many published article [9-14]. In this study, some phenylboronic acids are investigated which their structures are represented in Scheme 1. Ortho- and para- isomers are examined in detail. The whole investigations are performed by molecular simulation analyses. Ortho-substituent aryboronic acid are synthesized by Adamczyk-Wozniak and Sporzynski in 2020 [1].

The goal of this study is the investigating of the structural, spectral and non-linear optical (NLO) properties of mentioned compounds. All these compounds are optimized at M06–2X/6–311G(d) level in gas phase. Structural properties such as bond length, bond angle and geometry are revealed. Structural differences respect to location of substituent are reported in detail. IR and NMR spectrum are calculated for the spectral characterization of studied compounds. Vibration mode of selected peaks are analyzed with utilities. In NMR analyses, chemical shift values of carbon, hydrogen and boron atoms are reported. Molecular orbital energy diagram (MOED), contour plot of frontier molecular orbitals and molecular electrostatic potential (MEP) maps are examined to analyze the electronic properties. Finally, NLO properties are examined by using some parameters and UV–VIS spectrum. Urea is taken into consideration as reference material for the evaluating of the NLO properties of mentioned compounds.

2. Method

Computational analyses of selected phenylboronic acids were performed by licenced softwares. GaussView 6.0.16, Gaussian16 IA32W-G16RevB.01, Gaussian09 AS64L-G09RevD.01, ChemDraw Professional 15.1 and VEDA 4XX programs were used in this project [15-18]. Selected compounds were drawn by using GaussView and pre-optimizations were done by using Gaussian16 IA32W-G16RevB.01 at personal computer. Then, fully-optimizations were performed by using Gaussian09 AS64L-G09RevD.01 program at TR-Grid workstations. Universal force field (UFF) method was used in pre-optimizations while M06–2X/6–311G(d) level in gas phase. IR spectrum of studied phenylboronic acids were analyzed by VEDA 4XX program. gage-Independent Atomic Orbital (GIAO) method was used in the NMR calculations. As for the UV–VIS calculations, time-dependent (TD) method was used in the calculations. The total static dipole moment (μ), the average linear polarizability (α), the anisotropy of the polarizability ($\Delta\alpha$) and first hyperpolarizability (β) are calculated by using the Eq. (1) - (4):

* Corresponding author.
E-mail addresses: ksayin@cumhuriyet.edu.tr, krysayin@gmail.com (K. Sayin).

https://doi.org/10.1016/j.molstruc.2020.129550
0022-2860/

Compound ID	R_1	R_2	Compound ID	R_1	R_2
B1	-F	-H	B10	-H	-F
B2	$-CH_3$	-H	B11	-H	$-CH_3$
B3	-COH	-H	B12	-H	-COH
B4	$-OCH_3$	-H	B13	-H	$-OCH_3$
B5	$-OCH_2CH(CH_3)_2$	-H	B14	-H	$-OCH_2CH(CH_3)_2$
B6	$-NO_2$	-H	B15	-H	$-NO_2$
B7	$-CF_3$	-H	B16	-H	$-CF_3$
B8	-Ph	-H	B17	-H	-Ph
B9	$-CH_2N(CH_3)_2$	-H	B18	-H	$-CH_2N(CH_3)_2$

Scheme 1. Studied ortho- and para-substituted phenylboronic acid compounds.

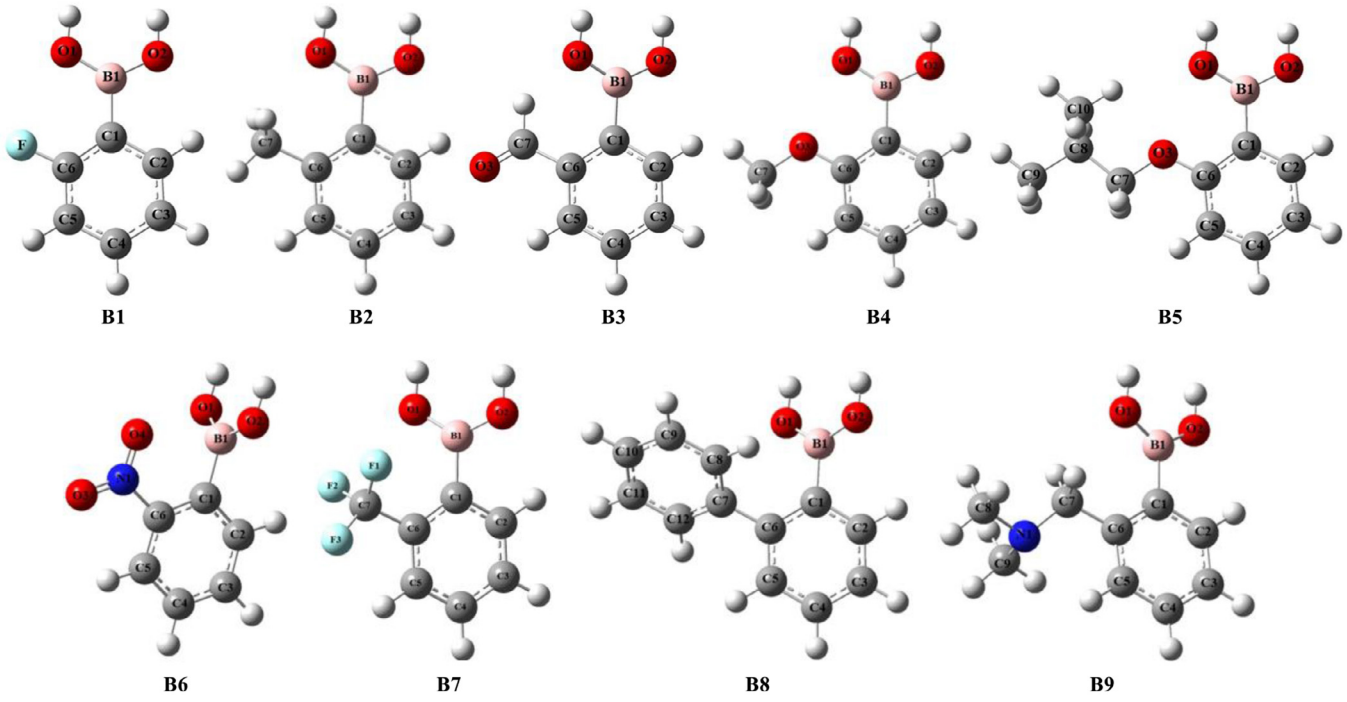

Fig. 1. The optimized structure of studied ortho-phenylboronic acid.

$$\mu = \sqrt{\mu_x^2 + \mu_y^2 + \mu_z^2} \quad (1)$$

$$\alpha = \frac{1}{3}(\alpha_{xx} + \alpha_{yy} + \alpha_{zz}) \quad (2)$$

$$\Delta a = \frac{1}{\sqrt{2}}\left[(a_{xx} - a_{yy})^2 + (a_{yy} - a_{zz})^2 + (a_{zz} - a_{xx})^2 + 6a_{xz}{}^2 + 6a_{xy}{}^2 + 6a_{yz}{}^2\right]^{1/2} \quad (3)$$

$$\beta = \left[(\beta_{xxx} + \beta_{xyy} + \beta_{xzz})^2 + (\beta_{yyy} + \beta_{xxy} + \beta_{yzz})^2 + (\beta_{zzz} + \beta_{xzz} + \beta_{yzz})^2\right]^{1/2} \quad (4)$$

3. Results and discussions

3.1. Structure and characterization

Studied compounds are optimized at mentioned level. Optimized structures of B1 – B9 are represented in Fig. 1 with atomic labeling. Structures of other compounds are represented at Supp. Fig. S1 – S9. Geometric parameters of B1-B9 are given in Table 1 while structural parameters of B10-B18 are given in Supp. Table S1.

According to Table 1, bond lengths of B1-C1 and B1-O1/2 are nearly calculated as 1.57 and 1.36 Å, respectively. According to published article, B-C and B-O bond lengths have been reported as 1.55 [19] and 1.38 Å [20]. So, calculated results are in agreement with published article. In carbon-carbon bonds, length of this bond in benzene ring is calculated about 1.39 Å. As experimentally, this bond has been reported as 1.38 Å [21, 22]. As for the bond angles, calculated the bond angle is nearly 120^0. Generally, planar structure is dominant in each compound.

In spectral analyses, IR spectrum of each compounds are calculated and analyzed by VEDA 4XX program. The calculated IR spectrum of B1 – B18 are represented in Supp Fig. S10-S27. The analysis results are given in Table 2 for B1-B9 and Supp. Table S2 for B10-B18.

According to Table 2, the vibration frequencies and their modes are reported in detail. While the stretching movement is generally dominant over 1500, it is determined that there are new movements such as torsion and out in addition to stretching in the fingerprint area. Functional groups such as hydroxyl and specific bonds belong to studied compounds are de-

Table 1
Calculated geometric parameters of B1-B9.

Assignment	B1	B2	B3	B4	B5	B6	B7	B8	B9
Bond Length (Å)									
B1-O1	1.361	1.365	1.363	1.363	1.364	1.361	1.359	1.363	1.365
B1-O2	1.365	1.369	1.362	1.372	1.370	1.361	1.362	1.366	1.367
B1-C1	1.572	1.573	1.578	1.572	1.572	1.586	1.579	1.574	1.573
C1-C6	1.391	1.411	1.407	1.411	1.410	1.391	1.403	1.408	1.410
C1-C2	1.403	1.402	1.401	1.399	1.399	1.397	1.398	1.400	1.402
C5-C6	1.386	1.397	1.397	1.399	1.399	1.388	1.391	1.398	1.396
C6-O3	–	–	–	1.355	1.353	–	–	–	–
C6-C7	–	1.510	1.489	–	–	–	1.504	1.487	1.520
C7-O3	–	–	1.210	1.416	1.421	–	–	–	–
Bond Angles (deg.)									
O1-B1-O2	121.4	122.9	124.3	122.6	122.7	125.7	124.8	124.0	123.3
O1-B1-C1	119.6	120.5	116.3	122.0	121.8	117.0	119.0	119.0	120.0
C1-C2-C3	120.4	122.1	121.6	122.5	122.5	121.3	121.7	121.7	122.0
C1-C6-C7	–	122.5	121.8	–	–	–	120.4	121.5	–
C1-C6-O3	–	–	–	117.0	116.8	–	–	–	–
C5-C6-C7	–	118.5	117.3	–	–	–	–	–	–
C6-O3-C7	–	–	–	118.4	119.3	–	–	–	–

Table 2
IR spectrum analyses of B1-B9.

Assignment	B1		B2		B3		B4		B5	
	Freq.[a]	Mode[b]	Freq.[a]	Mode[b]	Freq.[a]	Mode[b]	Freq.[a]	Mode[b]	Freq.[a]	Mode[b]
1	3884	STRE (OH)	3885	STRE (OH)	3881	STRE (OH)	3867	STRE (OH)	3889	STRE (OH)
2	3209	STRE (CH)	3193	STRE (CH)	3097	STRE (CH)	3054	STRE (CH)	3118	STRE (CH)
3	1693	STRE (CC)	1681	STRE (CC)	1808	STRE (OC)	1678	STRE (CC)	1674	STRE (CC)
4	1414	STRE (BO)	1399	STRE (BO)	1408	STRE (BO)	1405	STRE (BO)	1400	STRE (BO)
5	969	BEND (HOB)	967	BEND (HOB)	970	BEND (HOB)	989	TORS (HCCC)	1310	STRE (CC)
6	575	TORS (HOBC)	569	TORS (HOBC)	571	TORS (HOBC)	785	TORS (HCCC), TORS (CCCC), OUT (OCCC)	967	BEND (HOB)
7							566	TORS (HOBC)	789	TORS (HCCC), OUT (OCCC)
8									572	TORS (HOBC)
Assignment	B6		B7		B8		B9			
	Freq.[a]	Mode[b]	Freq.[a]	Mode[b]	Freq.[a]	Mode[b]	Freq.[a]	Mode[b]		
1	3878	STRE (OH)	3877	STRE (OH)	3878	STRE (OH)	3880	STRE (OH)		
2	3235	STRE (CH)	3216	STRE (CH)	3214	STRE (CH)	2986	STRE (CH)		
3	1662	STRE (CC)	1423	STRE (BO)	1676	STRE (CC)	1677	STRE (CC)		
4	1414	STRE (BO)	1185	STRE (FC)	1402	STRE (BO)	1397	STRE (BO)		
5	981	BEND (HOB)	977	BEND (HOB)	974	BEND (HOB)	972	BEND (HOB)		
6	557	TORS (HOBC)	578	TORS (HOBC)	554	BEND (OBO), TORS (HOBC)	553	TORS (HOBC)		

[a] in cm^{-1}.
[b] STRE: stretching; TORS: torsion; OUT: out of plane.

Table 3
The chemical shift values (in ppm) of carbon atoms in B1-B9.

Assignment	B1	B2	B3	B4	B5	B6	B7	B8	B9
C1	138.3	153.0	160.8	138.8	139.1	157.3	156.8	157.5	153.3
C2	160.2	159.0	158.2	160.8	160.4	153.9	157.8	156.6	158.6
C3	144.4	145.9	155.8	138.5	138.8	158.8	153.8	147.9	145.4
C4	155.3	152.5	152.4	155.5	154.7	150.4	151.3	151.6	152.6
C5	134.6	151.4	171.6	126.8	127.4	142.6	146.2	150.1	147.4
C6	189.1	171.0	162.1	186.4	185.8	171.0	154.6	171.7	171.9
C7		27.0	218.6	56.1	77.1		130.3	167.9	69.1
C8					32.5			152.1	49.5
C9					19.8			149.0	45.6
C10					21.4			148.3	
C11								149.7	
C12								148.8	

termined by IR spectrum analyses. The other significant characterization technique is NMR spectrum. NMR spectrum of studied compounds are calculated and chemical shift values of carbon and hydrogen atoms in B1-B9 are given in Table 3 and 4, respectively. The results in B10-B18 are given in Supp. Table S3 and S4.

According to Table 3 and 4, chemical shift values of aromatic carbon atoms are mainly calculated in the range of 138 – 186 ppm while chemical shift values of hydrogen atoms at benzene ring are mainly calculated in the range of 7.4 – 9.0 ppm. For hydrogen atoms which coordinate aliphatic carbon atoms, it is calculated in the range of 0.7 – 2.7 ppm. Finally, the chemical shift values

Table 4
The chemical shift values (in ppm) of hydrogen atoms in B1-B9.

Assignment	B1	B2	B3	B4	B5	B6	B7	B8	B9
C2*H*	8.8	9.0	9.1	8.9	8.9	8.4	8.8	8.8	8.9
C3*H*	8.0	8.1	8.6	7.9	7.8	8.6	8.5	8.3	8.3
C4*H*	8.5	8.4	8.5	8.3	8.4	8.6	8.7	8.4	8.4
C5*H*	7.7	8.0	9.1	7.4	7.4	9.0	8.6	8.4	8.6
C7*H*		3.1	11.5	3.7	4.2				4.2
C7*H*'		3.1		4.3	3.4				3.9
C7*H*"		2.3		3.7					
C8*H*					2.2			8.2	1.5
C8*H*'									2.5
C8*H*"									2.3
C9*H*					1.3			8.4	2.2
C9*H*'					1.2				2.6
C9*H*"					0.8				2.7
C10*H*					0.7			8.3	
C10*H*'					2.4				
C10*H*"					1.2				
C11*H*								8.6	
C12*H*								8.5	
O1*H*	4.3	4.0	4.4	3.8	4.0	4.3	4.4	4.2	4.2
O2*H*	4.1	4.1	4.5	4.1	3.9	4.3	4.4	3.7	4.1

of hydrogen atoms in hydroxyl group are obtained about 4.2 ppm. All these results are in agreement with theoretical expectation and published articles.

3.2. Contour Plots (CP) and molecular electrostatic potential (MEP) map

Molecular orbitals are significant illustration in the determination of properties of studied chemicals. The most known molecular orbitals are called as frontier molecular orbitals which are the highest occupied molecular orbital (HOMO) and the lowest unoccupied molecular orbital (LUMO) have the decision maker properties in the determination of interaction mechanism. In this stage, CPs of HOMO and LUMO give clues which are related with electron density on molecular structure. This electronic distribution provides the determination of the interaction mechanism. CPs of mentioned molecular orbitals in ortho substituted phenylboronic acid which are B1 – B9 are represented in Fig. 2. For the other compounds, contour plots of HOMO and LUMO are represented in Supp. Fig. S28.

According to Fig. 3, electrons in HOMO are mainly delocalized on the benzene ring. Therefore, it can be said that π electrons are active to any interactions. At the same time, there are small balloons on the oxygen atoms. It implies that oxygen atoms are active. However, their activities are less than benzene ring. As for the LUMO, the compounds can accept electrons from appropriate chemicals. These electrons will mainly be delocalized on the whole structure. Another important cube is molecular electrostatic potential (MEP) map and these maps for B1-B18 are represented in Fig. 3. For the other compounds, they are represented in Supp. Fig. S29.

MEP maps are obtained by the calculation of electro-static potential (ESP) charges. There are different colors in these maps. The red one implies the most electron density region while dark blue implies the most electron-less region. According to Fig. 3, red color is localized on the benzene ring and heteroatoms. The dark blue color is seen due to the hydrogen atoms. But it can be said that red and yellow colors is dominant on the structure and the electron delocalization is easily seen from MEP map. These results imply that studied compounds can be good candidates as optical materials.

3.3. Investigations of nonlinear optical (NLO) properties

Determination of optical properties of chemicals is significant topic for optical material. These properties can be determined by experimentally and computationally. For this investigation, UV–VIS spectrum and NLO parameters are used in this study. The wavelength of main band gives important data to evaluate the optical properties. It is known that electronic mobility is one of the parameters for the determination of NLO activity. The NLO activity increases with the increasing of wavelength of main band due to the fact that the wavelength and transition energy are inversely proportional. The wavelength of main bands of studied compounds are given in Table 5.

According to Table 5, the wavelength of ortho substituent studied compounds are mainly higher than that of para substituent ones. Therefore, it can be considered that electron mobility or electronic transitions are more in ortho substituent compounds. So, NLO activity of ortho substituent compounds which are B1-B9 are more than the others. In first nine compounds, the best candidate for NLO applications is B3 due to having highest wavelength. However, there are alternative compound to B3 because their wavelengths are close to B3's. The total static dipole moment (μ), the average linear polarizability (α), the anisotropy of the polarizability ($\Delta\alpha$) and first hyperpolarizability (β) are calculated for each compound and given in Table 6.

According to Table 6, NLO activity of the whole compounds is better than that of urea. However, there are some molecules that are thought to have better activity. Because, they have higher parameter values between each other. The first parameter is dipole moment. In this parameter, the NLO activity of B3, B12, B15 and B16 is better than the others. These compounds could be better NLO material. As a summary, these four compounds can be used as NLO material.

4. Conclusions

Phenylboronic acids are optimized at M062X/6–311G(d) at gas phase. Structural analyses of them are done in detail and charac-

Table 5
The wavelength (nm) of main bands and their oscillator stretching of each studied compound.

Compound	Wavelength	Osc. Stret.	Compound	Wavelength	Osc. Stret.
B1	175	0.541	B10	176	0.642
B2	179	0.657	B11	178	0.636
B3	190	0.353	B12	179	0.468
B4	182	0.672	B13	178	0.613
B5	183	0.628	B14	179	0.756
B6	157	0.348	B15	168	0.298
B7	176	0.635	B16	175	0.571
B8	188	0.377	B17	183	0.950
B9	181	0.424	B18	179	0.587

Table 6
Calculate NLO parameters of studied compounds.

Comp.	μ [1]	α [2]	$\Delta\alpha$ [2]	β [3]	Comp.	μ [1]	α [2]	$\Delta\alpha$ [2]	β [3]
B1	1.031	9.552	17.313	1.68×10^{-27}	B10	1.729	9.539	17.526	3.92×10^{-27}
B2	1.166	11.093	20.042	2.25×10^{-27}	B11	0.934	11.113	21.021	3.80×10^{-27}
B3	1.966	11.427	20.135	3.12×10^{-27}	B12	2.364	11.618	21.412	4.90×10^{-28}
B4	0.739	11.593	21.176	7.96×10^{-28}	B13	0.964	11.592	22.645	5.77×10^{-27}
B5	0.827	15.096	31.226	3.03×10^{-27}	B14	0.870	15.669	32.029	6.75×10^{-27}
B6	1.550	11.053	20.713	1.46×10^{-27}	B15	3.107	11.647	20.908	3.66×10^{-28}
B7	1.322	10.044	21.027	1.26×10^{-27}	B16	2.370	10.698	20.042	2.78×10^{-27}
B8	1.088	16.373	35.070	1.26×10^{-27}	B17	1.117	18.179	35.308	5.23×10^{-27}
B9	1.377	14.302	28.473	2.62×10^{-27}	B18	0.890	14.346	30.176	1.85×10^{-27}
Urea	0.172	2.290	9.144	3.84×10^{-28}					

[1] in Debye,
[2] in Å^3,
[3] in cm^5/esu.

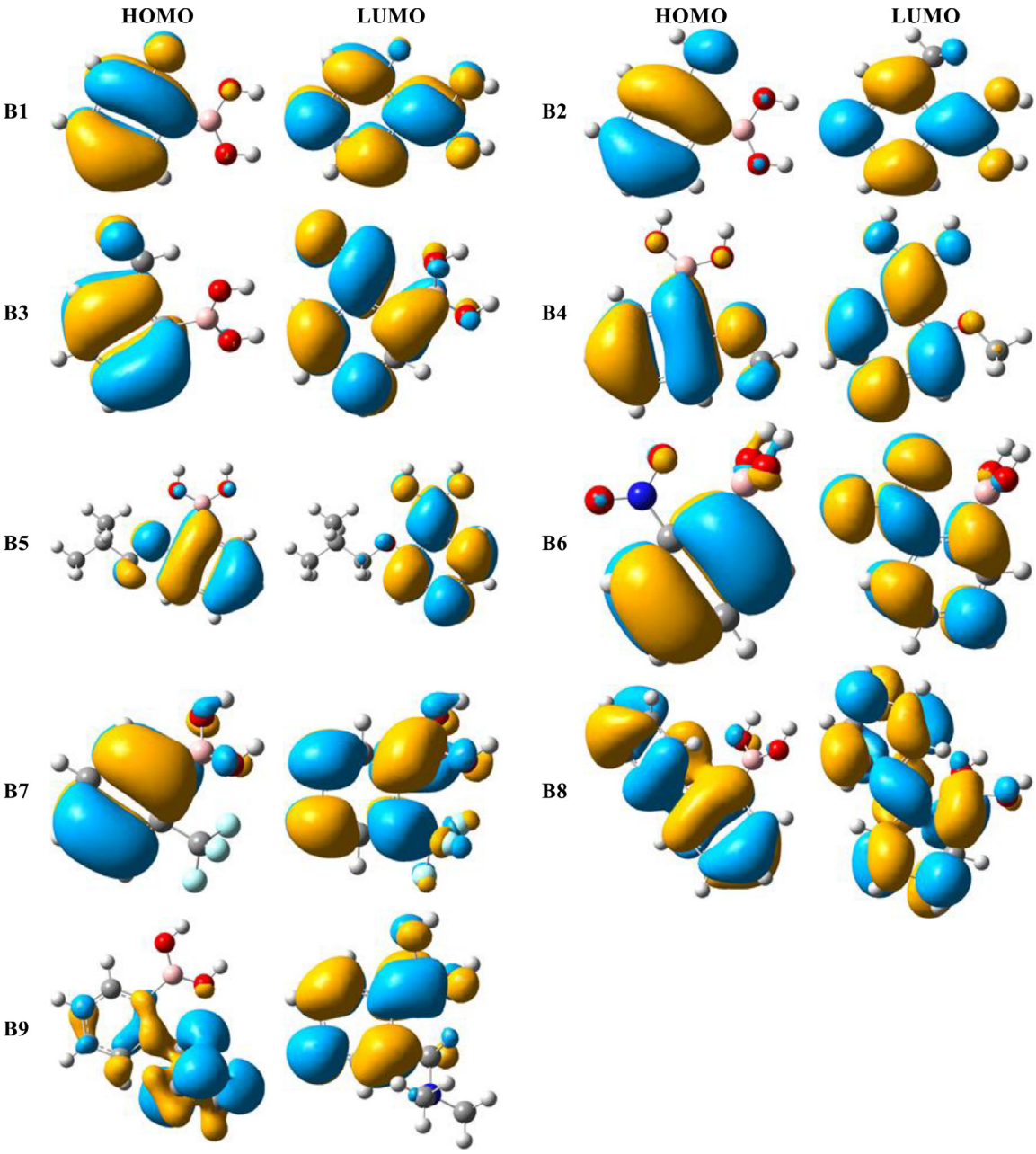

Fig. 2. Contour plots of frontier molecular orbitals of ortho substituent studied compounds.

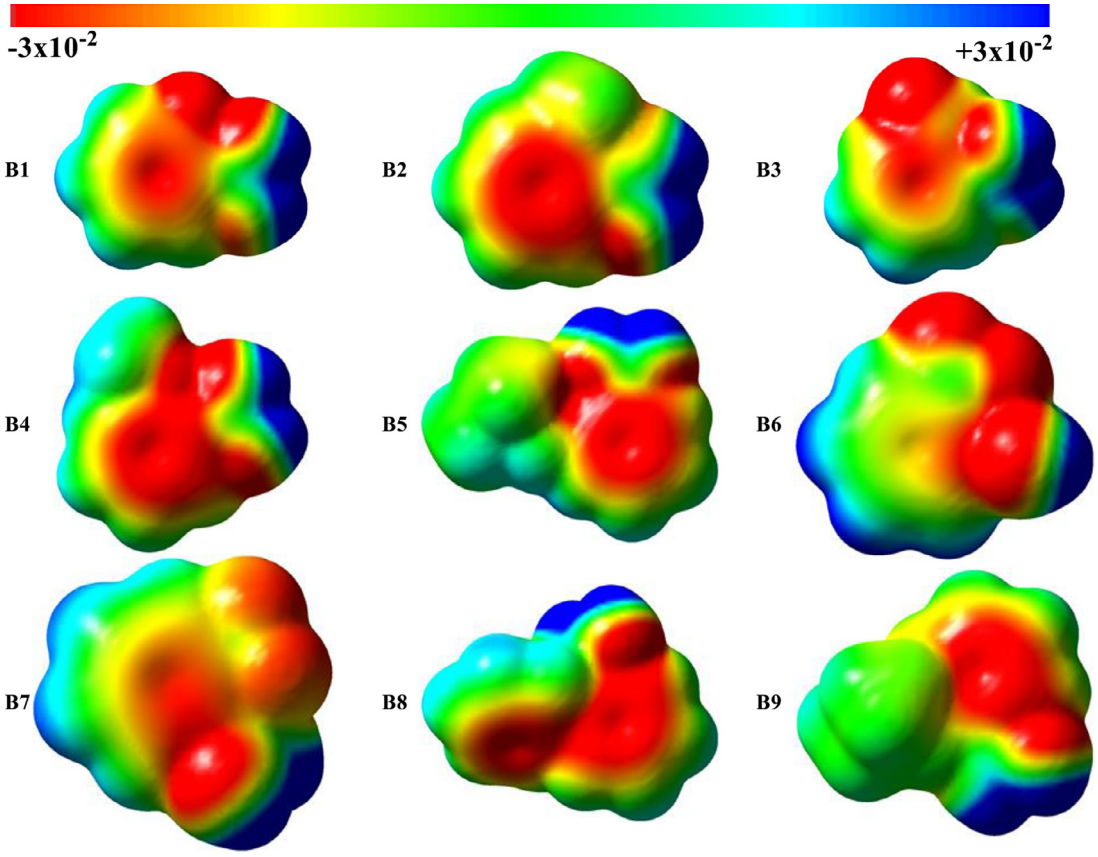

Fig. 3. The calculated MEP maps of studied compounds (B1-B9).

terization of these compounds are performed by calculating of IR and NMR spectrum. IR spectrum are analyzed by VEDA program. Additionally, contour plot of frontier molecular orbitals and molecular electrostatic potential (MEP) maps of them are obtained. So, electronic properties are revealed in detail. Finally, NLO properties of them are investigated. Initially, UV–VIS spectrum is calculated and the wavelength of main bands are examined in detail. Then, selected quantum chemical descriptors are calculated in evaluate the NLO activity of studied compounds. As a result, it is found that compounds which are B3, B12, B15 and B16 can be used as NLO material but it is determined that NLO efficiencies of B3 is more than those of other selected compounds.

Declaration of Competing Interest

The authors declare that they have no known competing financial interests or personal relationships that could have appeared to influence the work reported in this paper.

CRediT authorship contribution statement

Burcu Çöpçü: Investigation. **Koray Sayin:** Investigation, Writing - review & editing. **Duran Karakaş:** Investigation.

Acknowledgments

The numerical calculations reported in this paper were fully/partially performed at TUBITAK ULAKBIM, High Performance and Grid Computing Center (TRUBA resources).

Supplementary material

Supplementary material associated with this article can be found, in the online version, at doi:10.1016/j.molstruc.2020.129550.

References

[1] Agnieszka Adamczyk-Wozniak, Andrzej Sporzynski, The influence of ortho–substituents on the properties of phenylboronic acids, J. Organomet. Chem. 913 (2020) 121202.
[2] Jon S. Hansen, Thomas Hoeg-Jensen, Jørn B. Christensen, Redemitting BODIPY boronic acid fluorescent sensors for detection of lactate, Tetrahedron 73 (2017) 3010–3013.
[3] Verbitskiy E.V., Achelle S., Bures F., le Poul P., Barsella A., Kvashnin ˇ Y.A., Rusinov G.L., Guen FR-le, Chupakhin O.N., Charushin V.N., igSynthesis, photophysical and nonlinear optical properties of [1,2,5]oxadiazolo[3,4-*b*]pyrazine-based linear push-pull systems, J. Photochem. Amp; Photobiol., A (2020), 10.1016/j.jphotochem.2020.112900
[4] Rui Sun, Zhongxuan Qiu, Guorui Cao, Dawei Teng, Ni(II)/tBu-SMI-PHOX catalyzed enantioselective addition of arylboronic acids to cyclic N-sulfonyl aldimines, Tetrahedron 76 (2020) 131201.
[5] Jan Bartáček, Jiří Váňa, Pavel Drabina, Jan Svoboda, Martin Kocúrik, Miloš Sedlák, Recoverable polystyrene-supported palladium catalyst for construction of all-carbon quaternary stereocenters via asymmetric 1,4-addition of arylboronic acids to cyclic enones, React. Func. Polymers 153 (2020) 104615.
[6] Z. Bao, Z.-Y. Zhou, Y.-T. Mao, L.-X. Shao, N-heterocyclic carbene-Pd(II)-1-methylimidazole complex-catalyzed Suzuki-Miyaura coupling of 2-chloro-4-aminoquinazolines with arylboronic acids, Tetrahedron 76 (2020) 131–548.
[7] Sameeran Kumar Das, Mohendra Tahu, Minakshi Gohain, Dhanapati Deka, Utpal Bora, Bio-based sustainable heterogeneous catalyst for ipso-hydroxylation of arylboronic acid, Sust. Chem. Pharm. 17 (2020) 100296.
[8] Jian Liu, Menghang Ling, Hujun Xie, Mechanisms of chemoselectivity for acyl and decarbonylative Suzuki–Miyaura coupling of N-acetyl amide with arylboronic acid catalyzed by Pd and Ni catalysts: insights from DFT calculations, Comput. Theoretical Chem. 1185 (2020) 112889.
[9] Siyu Qian, Yuzhang Liang, Jie Ma, Yang Zhang, Jianzhang Zhao, Wei Peng, Boronic acid modified fiber optic SPR sensor and its application in saccharide detection, Sens. Actuators B 220 (2015) 1217–1223.
[10] Takao Mori, Thermoelectric and magnetic properties of rare earth borides: boron cluster and layered compounds, J. Solid State Chem. 275 (2019) 70–82.
[11] Nam Gwang Kim, Chang Hwan Shin, Min Hyung Lee, Youngkyu Do, Four-coordinate boron compounds derived from 2-(2-pyridyl)phenol ligand as novel hole-blocking materials for phosphorescent OLEDs, J. Organomet. Chem. 694 (2009) 1922–1928.

[12] Ahmet Karatay, Mustafa Yuksek, Hüseyin Ertap, Ali Kemal Mak, Mevlüt Karabulut, Ayhan Elmali, Influence of boron concentration on nonlinear absorption and ultrafast dynamics in GaSe crystals, Opt. Mater. (Amst) 60 (2016) 74–80.
[13] R. Mohandoss, B. Renganathan, O. Annalakshmi, A.R. Ganesan, Gamma radiation impact on the fiber optic acetone gas sensing behaviour of magnesium tetraborate, Opt. Fiber Technol. 52 (2019) 101935.
[14] Burak Tüzün, Koray Sayin, Investigations over optical properties of boron complexes of benzothiazolines, Spectrochimica Acta Part A 208 (2019) 48–56.
[15] R.D. Dennington II, T.A. Keith, J.M. Millam, GaussView 5.0, Wallingford, CT, 2009.
[16] M.J. Frisch, G.W. Trucks, H.B. Schlegel, G.E. Scuseria, M.A. Robb, J.R. Cheeseman, G. Scalmani, V. Barone, B. Mennucci, G.A. Petersson, H. Nakatsuji, M. Caricato, X. Li, H.P. Hratchian, A.F. Izmaylov, J. Bloino, G. Zheng, J.L. Sonnenberg, M. Hada, M. Ehara, K. Toyota, R. Fukuda, J. Hasegawa, M. Ishida, T. Nakajima, Y. Honda, O. Kitao, H. Nakai, T. Vreven, J.A. Montgomery Jr., J.E. Peralta, F. Ogliaro, M. Bearpark, J.J. Heyd, E. Brothers, K.N. Kudin, V.N. Staroverov, R. Kobayashi, J. Normand, K. Raghavachari, A. Rendell, J.C. Burant, S.S. Iyengar, J. Tomasi, M. Cossi, N. Rega, J.M. Millam, M. Klene, J.E. Knox, J.B. Cross, V. Bakken, C. Adamo, J. Jaramillo, R. Gomperts, R.E. Stratmann, O. Yazyev, A.J. Austin, R. Cammi, C. Pomelli, J.W. Ochterski, R.L. Martin, K. Morokuma, V.G. Zakrzewski, G.A. Voth, P. Salvador, J.J. Dannenberg, S. Dapprich, A.D. Daniels, O. Farkas, J.B. Foresman, J.V. Ortiz, J. Cioslowski, D.J. Fox, Gaussian09 AS64L-G09RevD.01, Gaussian, Inc, Wallingford CT, 2009.
[17] PerkinElmer, ChemBioDraw Ultra Version (15.1.0.144), CambridgeSoft Waltham, MA, USA, 2016.
[18] Michal..H. J.amroz, Vibrational Energy Distribution Analysis VEDA 4, Warsaw, 2004–2010.
[19] Nan Liu, Xiaoguang Luo, Xiaohong Yuan, Kun Luoa, Julong He, Dongli Yu, Yuanchun Zhao, Effect of the bond polarity on interlayer interactions in B–C–N layered materials: a dispersion-corrected density functional study, Mater. Today Commun. 22 (2020) 100781.
[20] Michael A. Beckett, David S. Brassington, Paul Owen, Michael B. Hursthouse, Mark E. Light, K.M. Abdul Malik, K. Sukumar Varma, p-Bonding in B–O ring species: lewis acidity of Me3B3O3, synthesis of amine Me3B3O3 adducts, and the crystal and molecular structure of Me3B3O3 . NH2 i Bu•MeB(OH)2, J. Organomet. Chem. 585 (1999) 7–11.
[21] Younes Valadbeigi, Effects of intramolecular hydrogen bond and electron delocalization on the basicity of proton sponges and superbases with benzene, pyridine, pyrazine and pyrimidine scaffolds, Comput. Theoretical Chem. 1188 (2020) 112947.
[22] Panaghiotis Karamanis, George Maroulis, Single (C–C) and triple (CBC) bond-length dependence of the static electric polarizability and hyperpolarizability of H–CC–CC–H, Chem. Phys. Lett. 376 (2003) 403–410.